

---

# ABC-GAN: Easy High-Dimensional Likelihood-Free Inference

---

Vinay Jethava, Devdatt Dubhashi

## Abstract

We introduce a framework using Generative Adversarial Networks (GANs) for likelihood-free inference (LFI) and Approximate Bayesian Computation (ABC) where we replace the black-box simulator model with an approximator network and generate a rich set of summary features in a data driven fashion. On benchmark data sets, our approach improves on others with respect to scalability, ability to handle high dimensional data and complex probability distributions.

## 1 Introduction

Approximate Bayesian Computation (ABC) is a likelihood-free inference method that learns the parameter  $\theta$  by generating simulated data  $\mathbf{Y}_\theta$  and accepting proposals (for the parameter  $\theta$ ) when the simulated data resembles the true data  $\mathbf{X}$  [see [Lintusaari et al., 2017](#), for a recent overview]. In most high-dimensional settings, a summary statistic  $T$  is chosen to represent the data so that the distance  $d(\mathbf{X}, \mathbf{Y}_\theta)$  can be computed in terms of the summary statistic  $d_T(t_{\mathbf{X}}, t_{\mathbf{Y}})$ . Rejection ABC [[Pritchard et al., 1999](#)] often suffers from low acceptance rates and several methods have been developed to address this problem. Broadly, these can be categorized as Markov Chain Monte Carlo methods [[Marjoram et al., 2003](#), [Beaumont et al., 2009](#), [Meeds et al., 2015](#), [Moreno et al., 2016](#)], sequential Monte Carlo [[Sisson et al., 2007](#)], and more recently, classifier-based approaches based on Bayesian optimization (BOLFI) [[Gutmann et al., 2016](#)].

In a series of recent papers, [Gutmann et al. \[2014, 2017, 2016\]](#) have suggested two novel ideas: (1) treating the problem of discriminating distributions as a classification problem between  $\mathbf{X}$  and  $\mathbf{Y}_\theta$ ; and (2) regression of the parameter  $\theta$  on the distance-measure  $d_T(\cdot, \cdot)$  using Gaussian Processes in order to identify the suitable regions of the parameter space having higher acceptance ratios.

This line of work is closely related to Generative Adversarial Networks (GANs) [[Goodfellow et al., 2014](#)] with different flavors of GANs [[Goodfellow et al., 2014](#), [Nowozin et al., 2016](#), [Arjovsky et al., 2017](#), [Dziugaite et al., 2015](#)] minimizing alternative divergences (or ratio losses) between the observed data  $\mathbf{X}$  and simulated data  $\mathbf{Y}_\theta$  [see [Mohamed and Lakshminarayanan, 2016](#), for an excellent exposition].

In this paper, we develop the connection between GANs [[Goodfellow, 2016](#)] and [Gutmann et al. \[2017\]](#) and present a new differentiable architecture inspired by GANs for likelihood-free inference (Figure 1). In doing so, we make the following contributions:

- We present a method for adapting black box simulator-based model with an “approximator”, a differentiable neural network module [similar to function approximation, see e.g., [Liang and Srikant, 2016](#), and references therein].
- Our method provides automatic generation of summary statistics as well as the choice of different distance functions (for comparing the summary statistics) with clear relation to likelihood ratio tests in GANs.
- We adapt one of the key ideas in [Gutmann et al. \[2017\]](#), namely, gradient-descent based search to quickly narrow down to the acceptance region of the parameter space, to the framework of GANs.

- We perform experiments on real-world problems (beyond Lotka-Volterra model) previously studied in the ABC literature - showing benefits as well as cases where the differentiable neural network architecture might *not* be the best solution (Section 4).

## 2 Related Work

**Summary statistics and distance function** The choice of summary statistic is known to be critical to the performance of the ABC scheme [Blum et al., 2013, Prangle, 2015]. Several methods have explored automatic generation of summary statistics, e.g., projection using regression [Fearhead and Prangle, 2012], random forests [Marin et al., 2016], etc. More recently, Prangle et al. [2017] have explored alternative distance functions for comparison of summary statistics. Within the classification scheme of [Prangle, 2015, Prangle et al., 2017], one of our contributions is automatic computation of non-linear projection-based summary statistics *and* a moment matching distance function (respectively, MMD [Dziugaite et al., 2015] or Wasserstein distance [Arjovsky et al., 2017]).

**LFI using neural networks** Several authors have recently proposed alternative approaches for likelihood-free inference [Meeds and Welling, 2015, Cranmer et al., 2015, Papamakarios and Murray, 2016, Tran et al., 2017]. In particular, Papamakarios and Murray [2016] inverted the ABC problem by sampling the parameter  $\theta$  from mixture of Gaussians  $q_\phi(\theta|\mathbf{x})$  (parametrized by neural network model  $\phi$ ). More recently, Tran et al. [2017] presented an elegant variational approach for likelihood-free inference under the restrictions that (1) the conditional density  $p(\mathbf{x}_n|\mathbf{z}_n, \theta)$  is indirectly specified as the hierarchical implicit model (similar to the “approximator” in this work) which given input noise  $\epsilon_n \sim s(\cdot)$  outputs sample  $\mathbf{x}_n$  given latent variable  $\mathbf{z}_n$  and parameter  $\theta$ , i.e.,  $\mathbf{x} \sim g(\epsilon|\mathbf{z}, \theta)$ ,  $\epsilon_n \sim s(\cdot)$ ; and (2) one can sample from the target distribution  $q(\mathbf{z}_n|\mathbf{x}_n, \theta)$ .

However, it is not clear how to extend these methods to the high-dimensional setting where choice of summary statistics is crucial. Further, the mean field assumption in [Tran et al., 2017] is not valid for time-series models. In contrast to above methods, this paper clearly demarcates the summarization from the approximation of the non-differentiable simulator. Additionally, not being constrained by a variational setup in [Tran et al., 2017], one can use sophisticated approximators/summarizer pairs for “simulating” a black-box simulator.

**Maximum Mean Discrepancy** The Maximum Mean Discrepancy (MMD) is an integral probability metric defined via a kernel  $k$  and its associated Reproducing Kernel Hilbert Space (RKHS) [Muandet et al., 2017, Sriperumbudur et al., 2012, Gretton et al., 2007]. Explicitly, the MMD distance with kernel  $k$  between distributions  $P$  and  $Q$  is given by  $MMD(k, P, Q) := E[k(X, \tilde{X})] - 2E[k(X, Y)] + E[k(Y, \tilde{Y})]$  where  $X, \tilde{X}$  are independent copies from  $P$  and  $Y, \tilde{Y}$  are independent copies from  $Q$ . For empirical samples  $X := \{x_1, \dots, x_m\}$  from  $P$  and  $Y := \{y_1, \dots, y_n\}$  from  $Q$ , an unbiased estimate of the MMD is  $\widehat{MMD}(k, X, Y) := \frac{1}{m(m-1)} \sum_{i,i'} k(x_i, x_{i'}) - \frac{2}{mn} \sum_{i,j} k(x_i, y_j) + \frac{1}{n(n-1)} \sum_{j,j'} k(y_j, y_{j'})$ . As shown in Dziugaite et al. [2015], this can be differentiated with respect to parameters generating one of the distributions.

## 3 Model

Let  $P(\mathbf{X}|\theta)$  denote a target distribution with unknown parameters  $\theta_0 \in \mathbb{R}^d$  that need to be estimated. We have access to a black box simulator  $S : (\theta, \epsilon) \rightarrow \mathbf{X}$  allowing us to generate samples from the distribution for any choice of parameter  $\theta$ . Here, we have captured the underlying stochasticity of the simulator using suitable noise  $\epsilon$ .

Figure 1 gives a high-level overview of the ABC-GAN architecture. The inputs to the network are the generator noise  $\beta$  and the simulator noise  $\epsilon$  which are problem-specific. The network functions

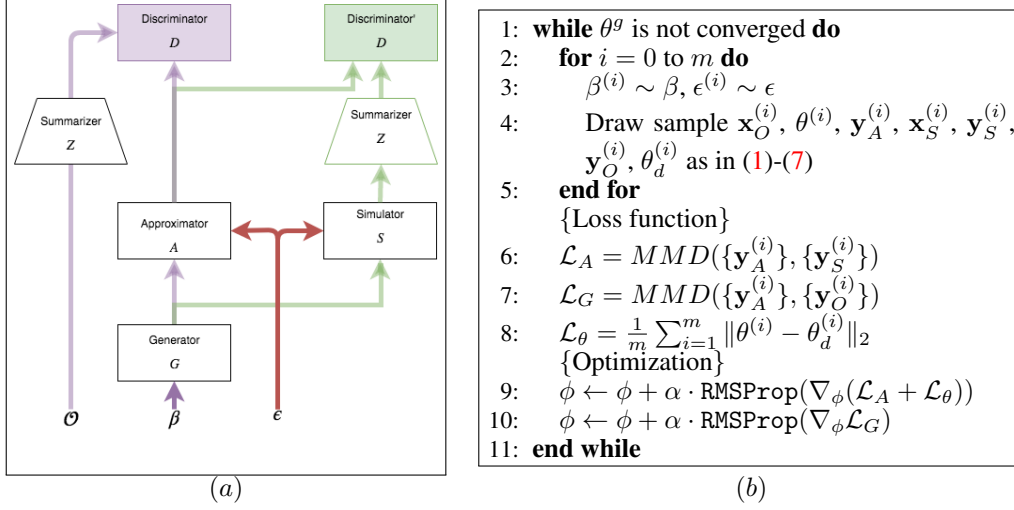


Figure 1: (a) ABC-GAN architecture for ABC computation. The external dependence on noise ( $\epsilon$ ) is shown in red. Two distinct network paths (shown in green and pink) correspond to two different optimizations (resp., *improve\_approx* and *improve\_accept*) akin to ratio test in GANs; (b) ABC-GAN implementation  $\alpha = 10^{-3}$ ,  $m = 50$ .

are given as

$$\mathbf{x}_O \sim \mathcal{O} \quad (\text{observations}) \quad (1)$$

$$\theta = G(\beta | \phi_G) \quad (\text{generator}) \quad (2)$$

$$\mathbf{y}_A = A(\theta, \epsilon | \phi_A) \quad (\text{approximator}) \quad (3)$$

$$\mathbf{x}_S = S(\theta, \epsilon) \quad (\text{simulator}) \quad (4)$$

$$\mathbf{y}_S = Z(\mathbf{x}_S | \phi_Z) \quad (\text{summary-sim.}) \quad (5)$$

$$\mathbf{y}_O = Z(\mathbf{x}_O | \phi_Z) \quad (\text{summary-obs.}) \quad (6)$$

$$\theta_d = A_d(\mathbf{y}_A | \phi_{A_d}) \quad (\text{decoder-approx.}) \quad (7)$$

The parameters are  $\phi = \{\phi_G, \phi_A, \phi_Z, \phi_{A_d}\}$  and the optimization consists of two alternating stages, namely:

- *improve\_approx*: This phase trains the approximator  $A$  and the summarizer  $Z$  against the black-box simulator using a ratio test between  $y_A$  and  $y_Z$ . Mathematically,

$$\min_{\phi_A, \phi_Z, \phi_{A_d}} \mathbb{E}_{\beta, \epsilon} [\mathcal{L}_A(\mathbf{y}_A, \mathbf{y}_S) + \mathcal{L}_\theta(\theta, \theta_d)]$$

where the loss term  $\mathcal{L}_\theta$  corresponds to a decoder for approximator  $A$  (as an encoding of parameter  $\theta$ ).

- *improve\_accept*: This phase trains the generator  $G$  in order to generate parameters that are similar to the observed data, i.e., with better acceptance rates. Mathematically,

$$\min_{\phi_G} \mathbb{E}_{\beta, \epsilon, \mathbf{x}_O \sim \mathcal{O}} [\mathcal{L}_G(\mathbf{y}_A, \mathbf{y}_O)]$$

The *improve\_approx* optimization (without *improve\_accept*) reduces to function approximation for the summary statistics of black-box simulator, with the decoder loss ensuring the outputs of the approximator and summarizer do not identically go to zero. A network as described above can be used in place of the simulator in a transparent fashion within an ABC scheme. However, this is extremely wasteful and the *improve\_accept* scheme incorporates gradient descent in parameter space to quickly reach the acceptance region similar to BOLFI [Gutmann et al., 2017]. Given the perfect approximator (or directly, the black-box simulator) and choosing an  $f$ -divergence [Nowozin et al., 2016, Mohamed and Lakshminarayanan, 2016] as loss  $\mathcal{L}_G$  ensures the generator unit attempts to produce parameters within the acceptance region.

Algorithm 1 shows our specific loss functions and optimization procedure used in this paper. In our experiments, we observed that training with MMD loss in lieu of the discriminator unit [Dziugaite et al., 2015] yielded the best results (Section 4).

**Discussion** We emphasize that our implementation (Algorithm 1) is just one possible solution in the ABC-GAN architecture landscape. For a new problem of interest, we highlight some of these choices below:

- *Pretraining* (*improve\_approx*): For a specific region of parameter space (e.g., based on domain knowledge), one can pre-train and fine-tune the approximator  $A$  and summarizer  $S$  networks by generating more samples from parameters within the restricted parameter space.
- *Automatic summarization*: Further, in domains where the summary statistic is not so obvious or rather adhoc (Section 4.2) - *improve\_approx* optimization provides a natural method for identifying good summary statistics.
- *Loss function/Discriminator*: Prangle et al. [2017] discuss why standard distance functions like Euclidean might not be suitable in many cases. In our architecture, the loss function can be selected based on the insights gained in the GAN community [Li et al., 2015, Bellemare et al., 2017, Arora et al., 2017, Sutherland et al., 2016].
- *Training*: GANs are known to be hard to train. In this work, *improve\_approx* is more crucial (since the approximator/summarizer pair tracks the simulator) and in general should be prioritized over *improve\_accept* (which chooses the next parameter setting to explore). We suggest using several rounds of *improve\_approx* for each round of *improve\_accept* in case of convergence problems.
- *Mode collapse*: We did not encounter mode collapse for a simple experiment on univariate normal (Supplementary Material, Section A). However, it is a known problem and an active area of research [Arjovsky et al., 2017, Arora et al., 2017] and choosing the Wasserstein distance [Arjovsky et al., 2017] has yielded promising results in other problems.
- *Module internals*: Our architecture is not constrained by independence between samples (vis-a-vis [Tran et al., 2017]). For example, in time series problems, it makes sense to have deep recurrent architectures (e.g., LSTMs, GRUs) that are known to capture long-range dependencies (e.g., Sections 4.2). Design of network structure is an active area of deep learning research which can be leveraged alongside domain knowledge.

## 4 Experiments

All experiments are performed using TensorFlow r1.3 on a Macbook pro 2015 laptop with core i5, 16GB RAM and *without* GPU support. The code for the experiments will be made available on github. In addition to experiments reported below, Section A in the supplementary material evaluates our ABC-GAN architecture on two small synthetic models, namely, univariate-normal and mixture of normal distributions.

### 4.1 Generalized linear model

Kousathanas et al. [2016] note that basic ABC algorithm and sequential Monte Carlo methods [Sisson et al., 2007, Beaumont et al., 2009] are useful for low-dimensional models, typically less than 10 parameters. To tackle higher dimensions, Kousathanas et al. [2016] consider scenarios where it is possible to define sufficient statistics for subsets of the parameters allowing parameter-specific ABC computation. This includes the class of exponential family of probability distributions.

In this example, we consider a generalized linear model defined by Kousathanas et al. [2016, Toy model 2] given as  $s = \mathbf{C}\theta + \epsilon$  where  $\theta \in \mathbb{R}^n$  denotes the unknown parameter,  $\epsilon$  denote multi-variate normal random variable  $\mathcal{N}(\mathbf{0}, \mathbf{I}_n)$  and  $\mathbf{C}$  is a design matrix  $\mathbf{C} = \mathbf{B} \cdot \det(\mathbf{B}^\top \mathbf{B})^{-\frac{1}{2n}}$  and

$$\mathbf{B} = \begin{bmatrix} \frac{1}{n} & \frac{2}{n} & \cdots & \frac{1}{n} \\ 1 & \frac{1}{n} & \cdots & \frac{n-1}{n} \\ \vdots & \vdots & \ddots & \vdots \\ \frac{2}{n} & \frac{3}{n} & \cdots & \frac{1}{n} \end{bmatrix}.$$

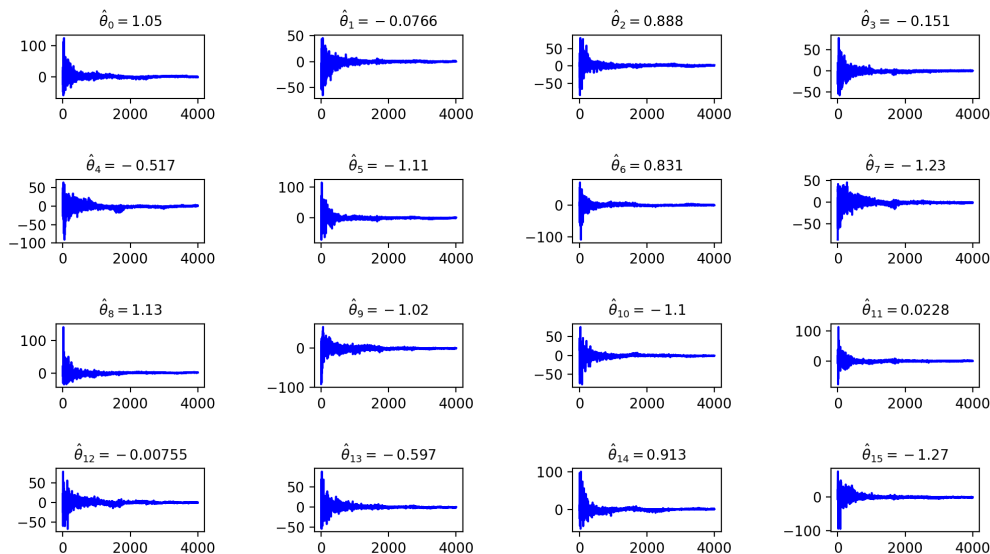


Figure 2: Inferred parameter values for one run of ABC-GAN for the GLM model (Section 4.1) with prior  $\theta_i \sim \text{Uniform}(-100, 100)$  and two layer feed-forward networks used for the generator and approximator in the ABC-GAN structure. The true parameter value is  $\mathbf{0}$ . We see that ABC-GAN algorithm recovers  $\hat{\theta}$  close to the true parameter  $\mathbf{0}$ .

We use a uniform prior  $\theta_i \sim \text{Uniform}(-100, 100)$  as in the original work. However, we note that [Kousathanas et al. \[2016\]](#) “start the MCMC chains at a normal deviate  $\mathcal{N}(\theta, 0.01\mathbf{I})$ , i.e., around the true values of  $\theta$ .” The true parameter is chosen as  $\theta = \mathbf{0}$ .

We do parameter inference for  $n = 16$  dimensional Gaussian in the above setting. Figure 2 shows the mean of the posterior samples within each mini-batch as the algorithm progresses<sup>1</sup>. The total number of iterations is 4000 with mini-batch size of 10 and learning rate of  $10^{-2}$ . The algorithm takes 10.24 seconds. We reiterate that ABC-GAN does not use model-specific information such as the knowledge of sufficient statistics for subsets of parameters, and thus, is more widely applicable than the approach of [Kousathanas et al. \[2016\]](#). Concurrently, it also enables computationally efficient inference in high-dimensional models – a challenge for Sequential Monte Carlo based methods [[Sisson et al., 2007](#), [Beaumont et al., 2009](#)] and BOLFI [[Gutmann et al., 2017](#)].

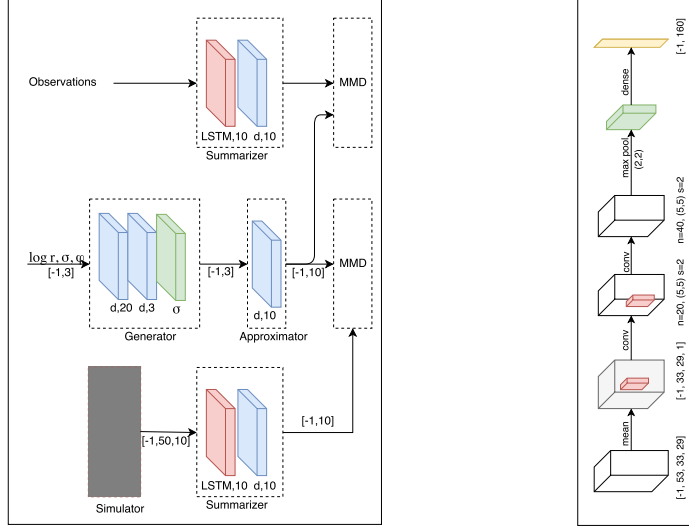
*In the high-dimensional setting, classic ABC methods or BOLFI cannot be easily used in contrast to this work.*

## 4.2 Ricker’s model

The stochastic Ricker model [[Ricker, 1954](#)] is an ecological model described by the nonlinear autoregressive equation:  $N^{(t)} = N^{(t-1)}r \exp(-N^{(t-1)} + \sigma e^{(t)})$  where  $N^{(t)}$  is the animal population at time  $t \in \{1, \dots, n\}$  and  $N^{(0)} = 0$ . The observation  $y^{(t)}$  is given by the distribution  $y^{(t)}|N^{(t)}, \phi \sim \text{Poisson}(\phi N^{(t)})$ , and the model parameters are  $\theta = (\log r, \sigma, \phi)$ . The latent time series  $N^{(t)}$  makes the inference of the parameters difficult.

[Wood \[2010\]](#) computed a synthetic log-likelihood by defining the following summary statistics: mean, number of zeros in  $y^{(t)}$ , auto-covariance with lag 5, regression coefficients for  $(y^{(t)})^3$  against  $[(y^{(t-1)})^3, (y^{(t-1)})^6]$ . They fit a Gaussian matrix to the summary statistics of the simulated samples and then, the synthetic log-likelihood is given by the probability of observed data under this Gaussian model. [Wood \[2010\]](#) inferred the unknown parameters using standard Markov Chain Monte

<sup>1</sup>For clarity, a larger version of this plot is presented in Figure 1 of the supplementary material.



(a) Network structure for Ricker model (b) Convolutional summarizer (DCC)

Figure 3: (a) Network structure of ABC-GAN for the Ricker model. Here,  $[d, 10]$ ,  $\sigma$  and  $LSTM, 10$  denote a densely connected layer with 10 outputs, sigmoid activation and a LSTM with 10 units respectively. (b) Convolutional summarizer for the DCC example. We generate summary representation consisting of 160 features from the input matrices  $I_{is}^{Tm}$ . The number of filters  $n$ , size of the filters (5, 5) and stride 2 are shown. The max\_pooling layer has size (2, 2). and the final dense layer outputs a summary representation of size 160 for each input sample.

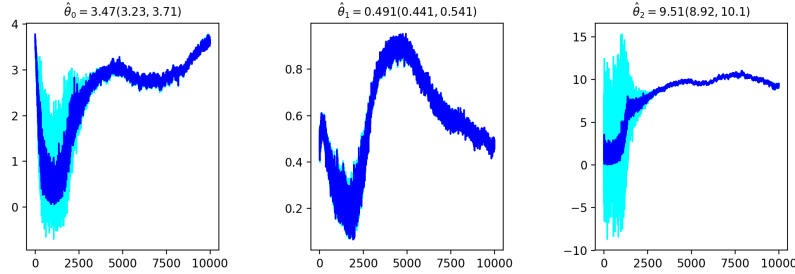


Figure 4: Inferred parameters for the Ricker model (Section 4.2) in a single run after 10000 iterations using  $RMSP_{\text{rop}}$  with learning rate= $10^{-3}$ , mini-batch size 10 and sequence length 10. The means of the estimated parameters for this run are (3.47, 0.49, 9.51) and the  $\pm 3\sigma$  range is shown.

Carlo (MCMC) method based on their synthetic log-likelihood. [Gutmann et al. \[2016\]](#) used the same synthetic log-likelihood but reduced the number of required samples for parameter inference based on regressing the discrepancy between simulated and observed samples (in terms of summary statistics) on the parameters using Gaussian Processes.

Figure 3 shows the network structure for the Ricker model <sup>2</sup> We follow the experimental setup of [Wood \[2010\]](#). We simulate observations from the Ricker model with true parameters (3.8, 0.3, 10). We use the following prior distributions:

$$\log r \sim \text{Uniform}(0, 5), \sigma \sim \text{Uniform}(0, 1), \phi \sim \text{Uniform}(0, 15).$$

Figure 4 shows the output of the generator (posterior samples for the parameters) for 10000 iterations of the algorithm. A mini-batch size of 10 is used with each sequence having length 10, and the optimization is done using  $RMSP_{\text{rop}}$  with a learning rate of  $10^{-3}$ . Figure 5 shows the histogram

<sup>2</sup>Please see the supplementary material for detailed description of the ABC-GAN architecture for the Ricker model.

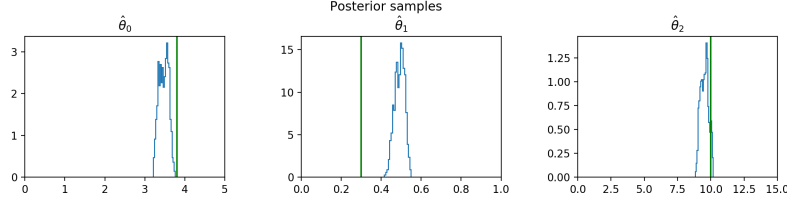


Figure 5: The histogram of the posterior samples for the last 1000 iterations of ABC-GAN in one run for the Ricker model. The true parameters (3.8, 0.3, 10) are shown in green.

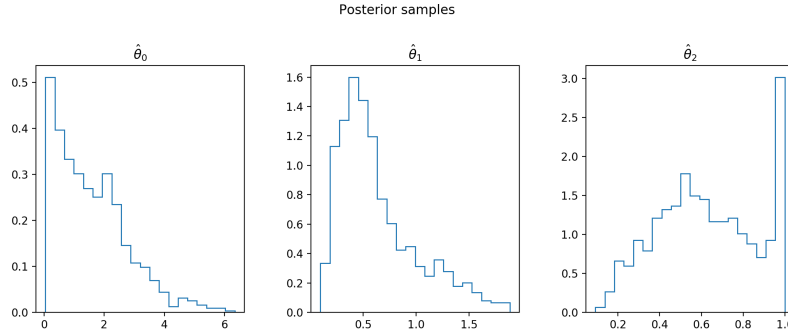


Figure 6: Result for the DCC example using the non-random features of Gutmann et al. [2017]. The true parameters are (3.6, 0.6, 0.1). A mini-batch size of 2 was used for 1000 iterations of the algorithm. The result shows the histogram of the posterior samples generated by the algorithm.

of the posterior samples for the last 1000 iterations of the algorithm. We note that the algorithm converges and is quite close to the true parameters.

We obtain the posterior means as  $(3.185 \pm 0.249, 0.677 \pm 0.077, 11.747 \pm 0.767)$  (averaged over 10 independent runs) for the number of true observations being  $N = 50$  and an typical time of 362 seconds for 10000 iterations. BOLFI estimates the following parameters (4.12, 0.15, 8.65) for  $N = 50$  data points [see Gutmann et al., 2016, Figure 9] and a typical run of BOLFI takes 300 seconds for the given setup<sup>3</sup>.

We re-emphasize that compared to the highly-engineered features of Wood [2010], our summary representation is learnt using a standard LSTM-based neural network [Hochreiter and Schmidhuber, 1997, Graves, 2012]. Thus, our approach allows for easier extensions to other problems compared to manual feature engineering.

*For complex simulators with latent variables (in a low-dimensional setting) with less number of observations and limited simulations, BOLFI performs best at significantly higher computational cost. Further, [Tran et al., 2017] is not suitable as mean field assumption is violated in the time-series model.*

### 4.3 Infection in Daycare center

We study the transmission of strains of *Streptococcus pneumoniae* in a total of 611 children attending one of 29 day care centers in Oslo, Norway. The initial data was published by Vestrheim et al. [2008] and further described in a follow-up study [Vestrheim et al., 2010]. Numminen et al. [2013] first presented an ABC-based approach for inferring the parameters associated with rates of infection from an outside source ( $\Lambda$ ), infection from within the DCC ( $\beta$ ) and infection by multiple strains ( $\theta$ ). Gutmann et al. [2017] presented a classification-based approach where they used classification as a surrogate for the rejection test of standard ABC method. Section C in the supplementary material presents a discussion of the hand-engineered features of Numminen et al. [2013] and Gutmann et al. [2017].

<sup>3</sup>The code provided by Dr. Michael Gutmann uses the GNU R and C code of Wood for synthetic log-likelihood and is considerably faster than the python version available in ELFI.

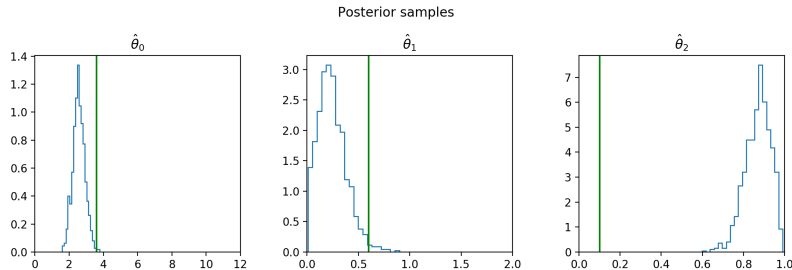


Figure 7: Histogram of the posterior samples generated by ABC-GAN for the DCC example using the convolutional summarizer. A learning rate of  $10^{-3}$  is used for 1000 iterations. The true parameters (3.6, 0.6, 0.1) are shown in green.

In the remainder of this section, we follow the nomenclature in [Gutmann et al., 2017]. For a single DCC, the observed data consists of presence or absence of a particular strain of the disease at time  $T^m$  when the swabs were taken. On average,  $N = 53$  individuals attend a DCC out of which only some are sampled. There are  $S = 33$  strains of the bacteria in total. So the data from each of the  $M = 29$  DCCs consists of a binary matrix with entries,  $I_{is}^t$  where  $I_{is}^t = 1$  if attendee  $i$  has strain  $s$  at time  $t$  and zero otherwise. The observed data  $\mathbf{X}$  consists of a set of  $M = 29$  binary matrices formed by  $I_{is}^{T_m}, i = 1, \dots, N_m, s = 1, \dots, 33$ . For the simulator, we use the code provided by Michael Gutmann which in turn uses the code of Elina Numminen <sup>4</sup>.

We assume the following prior on the parameters:

$$\Lambda \sim \text{Uniform}(0, 12), \beta \sim \text{Uniform}(0, 2), \theta \sim \text{Uniform}(0, 1).$$

We first use the non-random features defined by Gutmann et al. [2017] as our summary statistics. Figure 6 shows the histogram of the posterior samples generated by ABC-GAN using the non-random features defined by Gutmann et al. [2017]. We note that the results are not encouraging in this case, though this is an artifact of our algorithm. In order to address this, we define a new summary representation using a convolutional network. Figure 3 shows the structure of the convolutional summarizer which is used to generate summary representations instead of the non-random features defined by Gutmann et al. [2017]. The generator and approximator modules are standard one-layer feed forward networks which are fully described in Section C of the supplementary material.

Figure 7 shows the results for the convolutional summarizer. We note that the posterior samples improve especially for the parameters  $\Lambda = 3.6$  and  $\beta = 0.6$ . However, there is considerable room for improvement by using alternative summarization networks and improved training especially using more rounds of *improve\_approx* (for better approximation). We leave this to future work.

## 5 Conclusions

We present a generic architecture for training a differentiable approximator module which can be used in lieu of black-box simulator models without any need to reimplement the simulator. Our approach allows automatic discovery of summary statistics and crystallizes the choice of distance functions within the GAN framework. The goal of this paper is *not* to perform "better" than all existing ABC methods under all settings, rather to provide an easy recipe for designing scalable likelihood-free inference models using popular deep learning tools.

## References

- Martin Arjovsky, Soumith Chintala, and Léon Bottou. Wasserstein generative adversarial networks. In *International Conference on Machine Learning*, pages 214–223, 2017.
- Sanjeev Arora, Rong Ge, Yingyu Liang, Tengyu Ma, and Yi Zhang. Generalization and equilibrium in generative adversarial nets (gans). *CoRR*, abs/1703.00573, 2017. URL <http://arxiv.org/abs/1703.00573>.

<sup>4</sup><https://www.cs.helsinki.fi/u/gutmann/code/BOLFI/>



- Mark A Beaumont, Jean-Marie Cornuet, Jean-Michel Marin, and Christian P Robert. Adaptive approximate bayesian computation. *Biometrika*, 96(4):983–990, 2009.
- Marc G. Bellemare, Ivo Danihelka, Will Dabney, Shakir Mohamed, Balaji Lakshminarayanan, Stephan Hoyer, and Rémi Munos. The cramer distance as a solution to biased wasserstein gradients. *CoRR*, abs/1705.10743, 2017. URL <http://arxiv.org/abs/1705.10743>.
- Michael GB Blum, Maria Antonieta Nunes, Dennis Prangle, Scott A Sisson, et al. A comparative review of dimension reduction methods in approximate bayesian computation. *Statistical Science*, 28(2):189–208, 2013.
- Kyle Cranmer, Juan Pavez, and Gilles Louppe. Approximating likelihood ratios with calibrated discriminative classifiers. *arXiv preprint arXiv:1506.02169*, 2015.
- Gintare Karolina Dziugaite, Daniel M Roy, and Zoubin Ghahramani. Training generative neural networks via maximum mean discrepancy optimization. In *Proceedings of the Thirty-First Conference on Uncertainty in Artificial Intelligence*, pages 258–267. AUAI Press, 2015.
- Paul Fearnhead and Dennis Prangle. Constructing summary statistics for approximate bayesian computation: semi-automatic approximate bayesian computation. *Journal of the Royal Statistical Society: Series B (Statistical Methodology)*, 74(3):419–474, 2012.
- Ian Goodfellow. Nips 2016 tutorial: Generative adversarial networks. *arXiv preprint arXiv:1701.00160*, 2016.
- Ian Goodfellow, Jean Pouget-Abadie, Mehdi Mirza, Bing Xu, David Warde-Farley, Sherjil Ozair, Aaron Courville, and Yoshua Bengio. Generative adversarial nets. In *Advances in neural information processing systems*, pages 2672–2680, 2014.
- Alex Graves. *Supervised sequence labelling with recurrent neural networks*, volume 385. Springer, 2012.
- Arthur Gretton, Karsten M Borgwardt, Malte Rasch, Bernhard Schölkopf, and Alex J Smola. A kernel method for the two-sample-problem. In *Advances in neural information processing systems*, pages 513–520, 2007.
- Michael U Gutmann, Ritabrata Dutta, Samuel Kaski, and Jukka Corander. Statistical inference of intractable generative models via classification. *arXiv preprint arXiv:1407.4981*, 2014.
- Michael U Gutmann, Jukka Corander, et al. Bayesian optimization for likelihood-free inference of simulator-based statistical models. *Journal of Machine Learning Research*, 2016.
- M.U. Gutmann, R. Dutta, S. Kaski, and J. Corander. Likelihood-free inference via classification. *Statistics and Computing*, in press, March 2017. ISSN 1573-1375. doi: 10.1007/s11222-017-9738-6. URL <https://doi.org/10.1007/s11222-017-9738-6>.
- Sepp Hochreiter and Jürgen Schmidhuber. Long short-term memory. *Neural computation*, 9(8):1735–1780, 1997.
- Athanasios Kousathanas, Christoph Leuenberger, Jonas Helfer, Mathieu Quinodoz, Matthieu Foll, and Daniel Wegmann. Likelihood-free inference in high-dimensional models. *Genetics*, 203(2):893–904, 2016.
- Yujia Li, Kevin Swersky, and Richard S. Zemel. Generative moment matching networks. *CoRR*, abs/1502.02761, 2015. URL <http://arxiv.org/abs/1502.02761>.
- Shiyu Liang and R Srikant. Why deep neural networks for function approximation? *arXiv preprint arXiv:1610.04161*, 2016.
- Jarno Lintusaari, Michael U Gutmann, Ritabrata Dutta, Samuel Kaski, and Jukka Corander. Fundamentals and recent developments in approximate bayesian computation. *Systematic biology*, 66(1):e66–e82, 2017.
- Jean-Michel Marin, Louis Raynal, Pierre Pudlo, Mathieu Ribatet, and Christian P Robert. Abc random forests for bayesian parameter inference. *arXiv preprint arXiv:1605.05537*, 2016.

- Paul Marjoram, John Molitor, Vincent Plagnol, and Simon Tavaré. Markov chain monte carlo without likelihoods. *Proceedings of the National Academy of Sciences*, 100(26):15324–15328, 2003.
- Edward Meeds and Max Welling. Optimization monte carlo: Efficient and embarrassingly parallel likelihood-free inference. *CoRR*, abs/1506.03693, 2015. URL <http://arxiv.org/abs/1506.03693>.
- Edward Meeds, Robert Leenders, and Max Welling. Hamiltonian abc. *arXiv preprint arXiv:1503.01916*, 2015.
- Shakir Mohamed and Balaji Lakshminarayanan. Learning in implicit generative models. *arXiv preprint arXiv:1610.03483*, 2016.
- Alexander Moreno, Tameem Adel, Edward Meeds, James M Rehg, and Max Welling. Automatic variational abc. *arXiv preprint arXiv:1606.08549*, 2016.
- Krikamol Muandet, Kenji Fukumizu, Bharath Sriperumbudur, Bernhard Schölkopf, et al. Kernel mean embedding of distributions: A review and beyond. *Foundations and Trends® in Machine Learning*, 10(1-2):1–141, 2017.
- Sebastian Nowozin, Botond Cseke, and Ryota Tomioka. f-gan: Training generative neural samplers using variational divergence minimization. In *Advances in Neural Information Processing Systems*, pages 271–279, 2016.
- Elina Numminen, Lu Cheng, Mats Gyllenberg, and Jukka Corander. Estimating the transmission dynamics of streptococcus pneumoniae from strain prevalence data. *Biometrics*, 69(3):748–757, 2013.
- George Papamakarios and Iain Murray. Fast  $\epsilon$ -free inference of simulation models with bayesian conditional density estimation. In *Advances in Neural Information Processing Systems*, pages 1028–1036, 2016.
- Dennis Prangle. Summary statistics in approximate bayesian computation. *arXiv preprint arXiv:1512.05633*, 2015.
- Dennis Prangle et al. Adapting the abc distance function. *Bayesian Analysis*, 12(1):289–309, 2017.
- Jonathan K Pritchard, Mark T Seielstad, Anna Perez-Lezaun, and Marcus W Feldman. Population growth of human y chromosomes: a study of y chromosome microsatellites. *Molecular biology and evolution*, 16(12):1791–1798, 1999.
- William E Ricker. Stock and recruitment. *Journal of the Fisheries Board of Canada*, 11(5):559–623, 1954.
- Scott A Sisson, Yanan Fan, and Mark M Tanaka. Sequential monte carlo without likelihoods. *Proceedings of the National Academy of Sciences*, 104(6):1760–1765, 2007.
- Bharath K Sriperumbudur, Kenji Fukumizu, Arthur Gretton, Bernhard Schölkopf, Gert RG Lanckriet, et al. On the empirical estimation of integral probability metrics. *Electronic Journal of Statistics*, 6:1550–1599, 2012.
- Dougal J Sutherland, Hsiao-Yu Tung, Heiko Strathmann, Soumyajit De, Aaditya Ramdas, Alex Smola, and Arthur Gretton. Generative models and model criticism via optimized maximum mean discrepancy. *arXiv preprint arXiv:1611.04488*, 2016.
- Dustin Tran, Rajesh Ranganath, and David Blei. Hierarchical implicit models and likelihood-free variational inference. In *Advances in Neural Information Processing Systems*, pages 5529–5539, 2017.
- Didrik F Vestrheim, E Arne Høyby, Ingeborg S Aaberge, and Dominique A Caugant. Phenotypic and genotypic characterization of streptococcus pneumoniae strains colonizing children attending day-care centers in norway. *Journal of clinical microbiology*, 46(8):2508–2518, 2008.

Didrik F Vestrheim, E Arne Høyby, Ingeborg S Aaberge, and Dominique A Caugant. Impact of a pneumococcal conjugate vaccination program on carriage among children in norway. *Clinical and Vaccine Immunology*, 17(3):325–334, 2010.

Simon N Wood. Statistical inference for noisy nonlinear ecological dynamic systems. *Nature*, 466(7310):1102, 2010.

## Supplementary Material for ABC-GAN paper

**Contents**

<b>A Small-scale synthetic experiments</b>	<b>1</b>
A.1 Univariate normal distribution . . . . .	1
A.2 Mixture of normals . . . . .	2
A.3 Inference in multi-variate normal . . . . .	2
<b>B ABC-GAN specification for Ricker’s model</b>	<b>5</b>
<b>C Hand-engineered features for the DCC model</b>	<b>7</b>
<b>D ABC-GAN specification for the DCC model</b>	<b>7</b>
<b>E Supplemental Figures</b>	<b>8</b>

**A Small-scale synthetic experiments****A.1 Univariate normal distribution**

We generate  $N = 1000$  observations from the univariate normal distribution with mean  $\mu_0 = 3$  and variance  $\sigma_0^2 = 1$ . We use the following priors:

$$\mu \sim Unif(0, 5), \quad \sigma^2 \sim Unif(1, 5), \quad (1)$$

and perform parameter estimation ( $\hat{\mu}$  and  $\hat{\sigma}^2$ ) using rejection sampling, BOLFI and ABC-GAN. Table 1 shows the timing (in seconds) and accuracy results for the three approaches. We note that BOLFI is a complex method and is unsuited for this case since generation of univariate normal samples is computationally very cheap. Nonetheless, we observe that ABC-GAN converges in reasonable time and gives comparable results to others approaches.

*For low-dimensional problems with i.i.d. samples where simulation cost is cheap, classic ABC methods are best in terms of ease of implementation and wall-clock time.*

Method	$\hat{\mu}$	$\hat{\sigma}^2$	$t$ (in seconds)
ABC	2.92	1.17	0.147
BOLFI	2.68	1.13	2700
GAN	3.023	1.04	37.12

Table 1: We compare the results with naive ABC (using rejection sampling for 10000 samples) and BOLFI algorithm (Rejection sampling and ABC were implemented using ELFI [?]).

## A.2 Mixture of normals

We consider a mixture of two normal distributions, first studied in ?, with the observations generated from:

$$P_{\theta}(\theta) \sim \frac{1}{2}\mathcal{N}(0, \frac{1}{100}) + \frac{1}{2}\mathcal{N}(0, 1) \quad (2)$$

Here the second term implies large regions of low probability in comparison to the first term. Both classic rejection sampling and Monte Carlo ABC suffer from low acceptance rate and consequently, longer simulation runs (respectively, 400806 and 75895 steps) when generating samples from the low probability tail region.

In contrast, we run ABC-GAN for 5000 iterations with a mini-batch size of 10 and sequence length 10, using a learning rate  $10^{-3}$ .

Figure 1 shows the generated posterior samples and we see that the posterior samples capture the low probability component of the probability density function. We also run BOLFI [?] in order to compare its result to ABC-GAN.

Table 2 presents the timing and accuracy for the different methods. The accuracy is specified in terms of Kullback-Liebler divergence [?] between the true pdf and the empirical pdf estimated using posterior samples in the range  $[-10, 10]$ . We note that the KL-divergence of BOLFI w.r.t. true pdf is lower compared to the KL divergence of ABC-GAN w.r.t. true pdf. However, this does not translate to capturing the low-probability space as shown in Figure 1 (b) where BOLFI does not have samples in the low-dimensional space.

We note that BOLFI fails to adequately capture the low-probability space (due to the second component) of the problem. This is reflected in Table 2. Additionally, the BOLFI implementation in ELFI is considerably slower than ABC-GAN and this scenario is exacerbated as more number of observations are provided or more simulation samples are generated due to the use of Gaussian Processes.

## A.3 Inference in multi-variate normal

We consider multivariate normal model  $\mathbf{X} \in \mathbb{R}^{16}$  with true mean  $\mathbf{1}$  and prior on mean  $x_i \sim \text{Uniform}(0, 10)$ . We use two layer feed-forward neural networks as our generator and approximator units. A learning rate of  $10^{-3}$  and a hidden

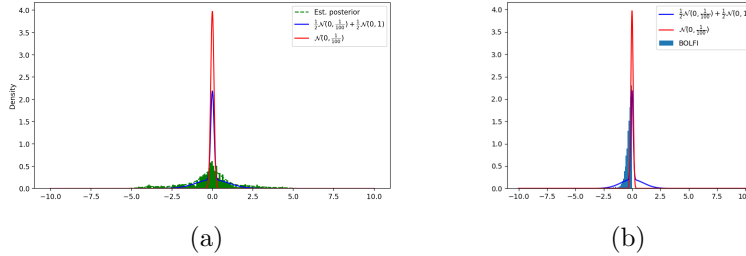


Figure 1: (a) Posterior samples for ABC-GAN (shown in green) for one run in the mixture of normals experiment (Section A.2) with 5000 iterations with a mini-batch size of 10 and sequence length 10, using a learning rate  $10^{-3}$ . The probability density function for the mixture normal and the low-variability component are shown in red and blue respectively. (b) Histogram of posterior samples for first run of BOLFI. Total number of samples is 5000. We note that the low-probability space is not captured by BOLFI compared to ABC-GAN.

Method	$n_s$	$D_{KL}(p  q)$	$t$
rej. sampl. <sup>†</sup>	5000	$0.567 \pm 0.012$	0.22
ABC-GAN	5000	$0.539 \pm 0.196$	14.70
BOLFI <sup>†</sup>	1000	$0.627 \pm 0.417$	126.71
BOLFI <sup>†</sup>	5000	$0.445 \pm 0.027$	426.03

Table 2: Timing and accuracy information for the mixture of normals example averaged over 10 independent runs. The the number of samples generated by the simulator ( $n_s$ ) are shown. The Kullback-Liebler divergence ( $D_{KL}(p||q)$ ) between the true pdf ( $p$ ) and the empirical pdf estimated using accepted samples ( $q$ ) and the time taken (for the first run) in seconds ( $t$ ) are shown. <sup>†</sup>ELFI returns only negative samples so we add  $-x$  to the samples for each original sample  $x$  before computing the KL divergence.

layer of size 16 is used in the approximator and generator units. MMD Loss is used as a surrogate for the discriminator as well as for comparing the output of the approximator unit with the simulator.

Figures 2 and 3 show the inferred parameters and the L1-loss between the inferred mean and the true mean as the algorithm progresses. We note that the inferred parameters are close to the true mean  $\mathbf{1}$ . The total time taken is 46.38 seconds.

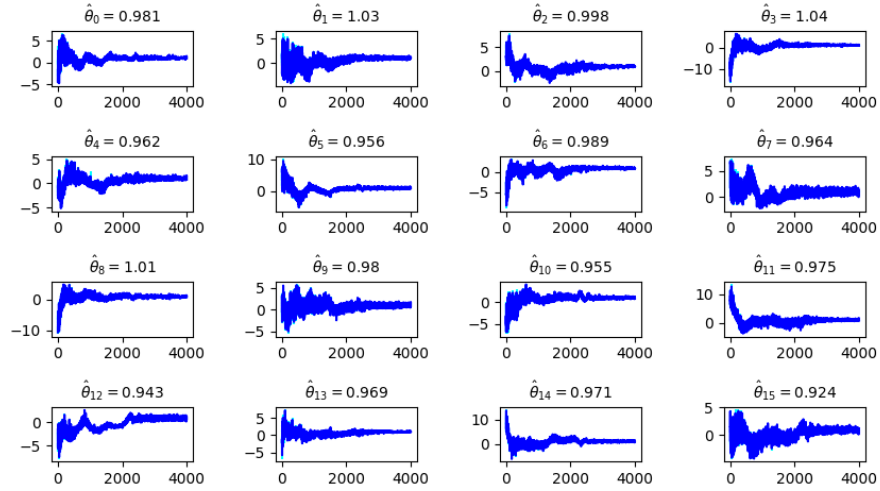


Figure 2: Inferred parameters for one run of ABC-GAN for the multi-variate normal model (Section A.3). We see that the inferred parameters are close to the true mean  $\mathbf{1}$ .

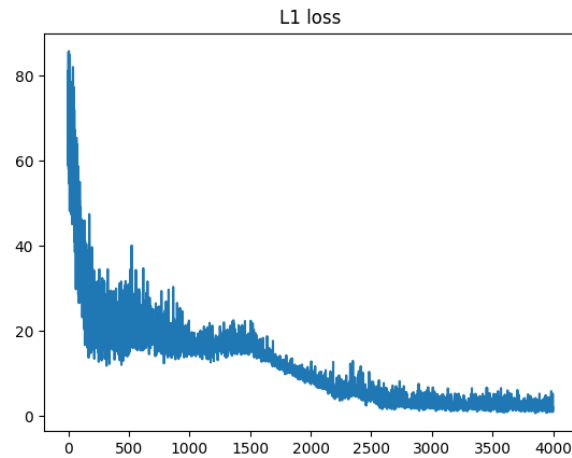


Figure 3: The L1-loss between the inferred and the true mean in the multi-variate normal example (Section A.3) as the algorithm progresses.

## B ABC-GAN specification for Ricker’s model

This section presents the complete model specification of our GAN architecture for the Ricker’s model. We describe each of the individual sub-networks below.

For sake of completeness, we recall the prior distribution on the parameters  $\theta = (\log r, \sigma, \phi)$  given by:

$$\begin{aligned}\log r &\sim \text{Uniform}(0, 5), \\ \sigma &\sim \text{Uniform}(0, 1), \\ \phi &\sim \text{Uniform}(0, 15).\end{aligned}$$

In the remainder of this section, the notation ( $d = 10$ ) indicates the layer has 10-dimensional output.

**Generator** The generator  $G_u(\cdot)$  takes as input the samples from the prior distribution on  $\theta = (\log r, \sigma, \phi)$ . The generator has the following equations:

$$\begin{aligned}x_{G,1} &= \text{ReLU}(w_{g,1}^\top \theta + b_{g,1}) & (d = 20) \\ x_{G,2} &= w_{u,2}^\top x_{g,2} + b_{g,2} & (d = 3) \\ x_{G,3} &= 5 \times \text{Sigmoid}(x_{G,2}[:, 1]) & (d = 1) & (\hat{\log r}) \\ x_{G,4} &= \text{Sigmoid}(x_{G,2}[:, 2]) & (d = 1) & (\hat{\sigma}) \\ x_{G,5} &= 15 \times \text{Sigmoid}(x_{G,2}[:, 3]) & (d = 1) & (\hat{\phi}) \\ x_G &= [x_{G,3}, x_{G,4}, x_{G,5}] & (d = 3) & (\hat{\theta}_{post})\end{aligned}$$

The complete set of weights are given by  $W_G = \{w_{g,i}, b_{g,i} \forall i \in 1, 2\}$  which are initialized using samples from the normal distribution  $\mathcal{N}(0, 1)$ .

**Approximator** The approximator unit consists of a feed-forward layer which takes as input the posterior parameters  $x_G$  from the generator and outputs approximate statistics given as:

$$x_A = w_{a,1}^\top x_G + b_{a,1} \quad (d = 3)$$

where the weights  $W_A = \{w_{a,1}, b_{a,1}\}$  are initialized from the normal distribution  $\mathcal{N}(0, 1)$ .

**Summarizer** The summarizer unit consists of LSTM cell followed by a dense layer which projects the sequence to the summary representation. We recall that the standard LSTM unit is defined as:

$$\begin{aligned}f_t &= \sigma(W_f \cdot [h_{t-1}, x_t] + b_f) & (\text{forget gate}) \\ i_t &= \sigma(W_i \cdot [h_{t-1}, x_t] + b_i) & (\text{input gate}) \\ \tilde{C}_t &= \tanh(W_c \cdot [h_{t-1}, x_t] + b_c) \\ C_t &= f_t * C_{t-1} + i_t * \tilde{C}_t & (\text{cell state}) \\ o_t &= \sigma(W_o \cdot [h_{t-1}, x_t] + b_o) & (\text{output}) \\ h_t &= o_t * \tanh(C_t)\end{aligned}$$



where  $W_{LSTM} = \{W_f, W_i, W_C, W_o, b_f, b_i, b_C, b_o\}$  are the weights for a single unit. We use the notation  $LSTM_k$  to denote  $k$  LSTM units connected serially.

Given input sequence  $seq$  obtained from the simulator or from observed data, the summarizer output is given by:

$$\begin{aligned} x_{S,1} &= LSTM_k(seq) & (d = k = 10) \\ x_S &= w_{s,1}^\top x_{S,1} + b_{s,1} & (d = 10) \end{aligned}$$

where the weights are given by  $W_S = \{w_{S,1}, b_{S,1}\} \cup w_{LSTM}$ . The weights are initialized to normal distribution and the initial cell state is set to zero tuple of appropriate size.

**Optimization** The connections are described as follows:

$$\begin{aligned} x_G &= \mathcal{G}(\theta; W_G) \\ x_A &= \mathcal{A}(x_G; W_A) \\ \mathbf{seq}_S &= \mathbf{simulator}(x_G, \epsilon) \\ x_S &= \mathcal{S}(\mathbf{seq}_S; W_S) \\ x_O &= \mathcal{S}(\mathbf{seq}_O; W_S) \end{aligned}$$

where  $\mathbf{seq}_O$  denotes the observed data,  $x_O$  is its summary representation obtained using the summarizer, and  $\epsilon$  denotes normal noise for input to the simulator alongwith the posterior parameter  $X_G$ .

We use maximum mean discrepancy (MMD) loss [?] to train the network. Given reproducing kernel Hilbert space (RKHS)  $\mathcal{H}$  with associated kernel  $k(\cdot, \cdot)$  and data  $X, X', X_1, \dots, X_N$  and  $Y, Y', Y_1, \dots, Y_M$  from distributions  $p$  and  $q$  respectively, the maximum mean discrepancy loss is given by:

$$MMD^2[\mathcal{H}, p, q] = E[k(X, X') - 2k(X, Y) + k(Y, Y')].$$

We use the Gaussian kernel and define the following loss functions:

$$\begin{aligned} \mathcal{L}_G &= MMD(x_A, x_O) \\ \mathcal{L}_R &= MMD(x_A, x_S) \end{aligned}$$

Let  $W_R = (W_S, W_A)$  denote the combined weights for the summarizer and the approximator units. The update equations for the network are then given by the following alternating optimizations:

$$\begin{aligned} W_R^{(i+1)} &\leftarrow W_R^{(i)} + \alpha \cdot \text{RMSProp}(\nabla_{W_A, W_S} \mathcal{L}_R) \\ W_G^{(i+1)} &\leftarrow W_G^{(i)} + \alpha \cdot \text{RMSProp}(\nabla_{W_G} \mathcal{L}_R) \end{aligned}$$

where  $\alpha$  is the learning rate for the RMSProp algorithm.

## C Hand-engineered features for the DCC model

? defined four summary statistics per day care center in order to characterize the simulated and observed data and perform ABC-based inference of the parameters  $\Theta = (\Lambda, \beta, \theta)$ :

- The strain diversity in the day care centers,
- The number of different strains circulating,
- The fraction of the infected children,
- The fraction of children infected with multiple strains.

? classified the simulated data as being fake (not having the same distribution as the observed data) or based on the following features:

1.  $L2$ -norm of the singular values and the rank of the original matrix (2 features),
2. The authors computed the fraction of ones in the set of rows and columns of the matrix. Then, the average and the variability of this fraction was taken across the whole set of rows and columns. Since the average is the same for the set of rows and columns, this yields 3 features.
3. The same features as (2) above for a randomly chosen sub-matrix having 10% of the elements of the original matrix (2 features).

By choosing 1000 random subsets, the authors converted the set of 29 matrices to a set of 1000 seven-dimensional features. This feature set was used to perform classification using LDA. They also did the classification without the randomly chosen subsets mapping each simulated dataset to a five-dimensional feature vector.

## D ABC-GAN specification for the DCC model

This section presents the complete description for our architecture doing likelihood free inference in the Daycare center example. We describe each of the sub-networks below.

**Generator** The generator  $\mathcal{G}(\cdot)$  takes as input the samples from the prior distribution on  $\Theta = (\Lambda, \beta, \theta)$ . It is specified as follows:

$$\begin{aligned}x_{G,1} &= w_{g,1}^\top \Theta + b_{g,1} & (d = 3) \\ \hat{\Lambda} &= 12 \cdot \sigma(x_{G,1}[:, 0]) & (d = 1) \\ \hat{\beta} &= 2 \cdot \sigma(x_{G,1}[:, 1]) & (d = 1) \\ \hat{\theta} &= \sigma(x_{G,1}[:, 2]) & (d = 1) \\ x_G &= [\hat{\Lambda} \hat{\beta} \hat{\theta}] & \end{aligned}$$

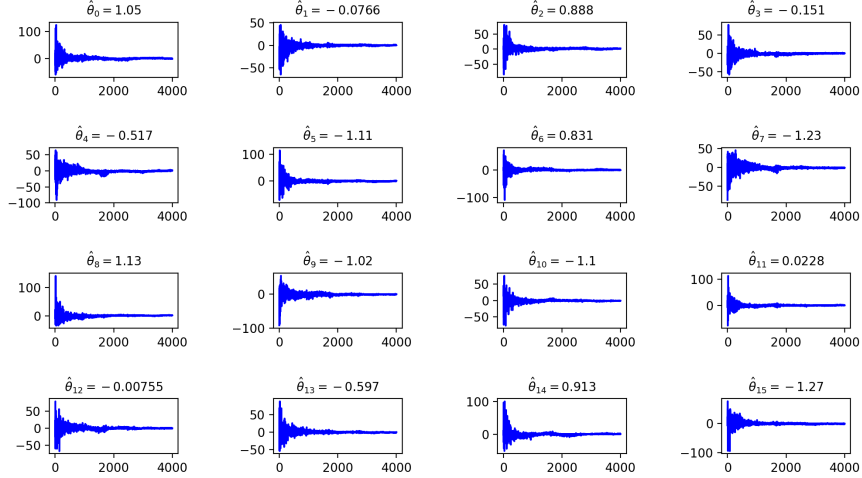


Figure 4: Inferred parameter values (true parameter is  $\mathbf{0}$ ) with prior  $\theta_i \sim \text{Uniform}(-100, 100)$  and two layer feed-forward networks used for the generator and approximator in the ABC-GAN structure.

The set of variables are given by  $W_G = [w_{g,1}, b_{g,1}]$  which are initialized using normal distribution.

**Approximator** The approximator unit has a feed-forward network given by:

$$x_A = w_{a,1}^\top x_G + b_{a,1}$$

where  $W_A = [w_{a,1}, b_{a,1}]$  are the weights which are initialized using the normal distribution.

## E Supplemental Figures

- Figure 4 shows the inferred parameter values in Section 4.1.3 of the main manuscript. The true parameter is  $\mathbf{0}$  with prior  $\theta_i \sim \text{Uniform}(-100, 100)$  and two layer feed-forward networks used for the generator and approximator in the ABC-GAN structure.